Shigella reroutes host cell central metabolism to obtain high-flux nutrient supply for vigorous intracellular growth

David Kentner[a,1,2], Giuseppe Martano[b,1], Morgane Callon[a,1], Petra Chiquet[a], Maj Brodmann[a], Olga Burton[a], Asa Wahlander[c], Paolo Nanni[c], Nathanaël Delmotte[b], Jonas Grossmann[c], Julien Limenitakis[a], Ralph Schlapbach[c], Patrick Kiefer[b], Julia A. Vorholt[b], Sebastian Hiller[a], and Dirk Bumann[a,2]

[a]Biozentrum, University of Basel, 4056 Basel, Switzerland; [b]Institute of Microbiology, Eidgenössiche Technische Hochschule Zürich, 8093 Zürich, Switzerland; and [c]Functional Genomics Center Zurich, 8057 Zürich, Switzerland

Edited by Philippe J. Sansonetti, Institut Pasteur, Paris, France, and approved May 28, 2014 (received for review April 16, 2014)

Shigella flexneri **proliferate in infected human epithelial cells at exceptionally high rates. This vigorous growth has important consequences for rapid progression to life-threatening bloody diarrhea, but the underlying metabolic mechanisms remain poorly understood. Here, we used metabolomics, proteomics, and genetic experiments to determine host and *Shigella* metabolism during infection in a cell culture model. The data suggest that infected host cells maintain largely normal fluxes through glycolytic pathways, but the entire output of these pathways is captured by *Shigella*, most likely in the form of pyruvate. This striking strategy provides *Shigella* with an abundant favorable energy source, while preserving host cell ATP generation, energy charge maintenance, and survival, despite ongoing vigorous exploitation. *Shigella* uses a simple three-step pathway to metabolize pyruvate at high rates with acetate as an excreted waste product. The crucial role of this pathway for *Shigella* intracellular growth suggests targets for antimicrobial chemotherapy of this devastating disease.**

infectious diseases | host–pathogen interactions

Infectious diseases typically arise when pathogens grow to high tissue loads, causing extensive damage and immunopathology. An outstanding example is *Shigella flexneri*, which rapidly grow from a small infectious dose of 10–100 bacteria (1) to intestinal loads causing life-threatening bloody diarrhea (bacillary dysentery) within a few hours (2, 3). This vigorous *Shigella* growth occurs inside human colon epithelial cells and requires an integrated *Shigella* pathogenesis program, including a type three secretion system encoded on the *Shigella* virulence plasmid. Using this system, *Shigella* translocates enzymes into the host cell cytosol, where they target key cellular functions, allowing *Shigella* to enter the host cell and escape bacterial killing by innate immune responses (4). After *Shigella* reaches the host cell cytosol, many virulence factors are down-regulated (5), and *Shigella* starts rapid proliferation.

Biomass generation at such high rates depends on extensive exploitation of intracellular host nutrients (6). The host cell cytoplasm contains hundreds of metabolites, but it is unclear which of these potential nutrients *Shigella* uses, how the host cell can supply them at sufficiently high rates to support rapid *Shigella* growth, and why host cells can sustain viability while being vigorously exploited by intracellular *Shigella*. For related enteroinvasive *Escherichia coli*, previous research has shown that glucose and other host metabolites, such as diverse amino acids, can be incorporated into the biomass of these closely related pathogens (7). However, quantitative data are still lacking, and energy production, which is usually a major part of nutrient use (8), could not be analyzed because of technical limitations.

In general, pathogen metabolism has been recognized as a fundamentally important aspect of infectious diseases, but available data are mostly restricted to qualitative presence/absence of enzymes in pathogen genomes and metabolite or gene expression profiles in various infection models (9–13). Comprehensive quantitative studies on pathogen nutrition, metabolism, and growth are largely lacking. This limited knowledge reflects, in part, the fact that suitable methodologies are just becoming available. In this study, we combined various metabolomics approaches, proteomics, and microbial genetics to elucidate the metabolic basis of *Shigella* rapid growth in infected human host cells.

Results

Shigella **Grow Rapidly Inside HeLa Host Cells.** We infected HeLa epithelial cells with *S. flexneri* 2a 2457T *icsA*. The *icsA* mutation prevents spread between host cells (14, 15), thereby simplifying analysis of intracellular growth. In this model, *Shigella* grew rapidly with a generation time of 37 ± 4 min (Fig. S1 and Movie S1), close to maximal axenic growth rates in rich broth and faster than almost all other pathogens in their respective host environments. Infected HeLa cells remained intact until around 3.5–4 h postinfection, when their cytoplasm was packed with more than 100 *Shigella*. The HeLa cells subsequently detached and disintegrated, which was observed previously (16).

Host Central Metabolism Remains Functional During *Shigella* Infection. Rapid intracellular *Shigella* growth likely causes a substantial

Significance

Shigella **causes devastating bloody diarrhea. Rapid disease progression results from exceptionally fast *Shigella* growth inside human gut epithelial cells, but how *Shigella* can obtain nutrients at such high rates from its host cell has been unclear. Here, we show that infected host cells maintain normal central metabolism for energy production and host cell survival. However, *Shigella* captures the entire host metabolism output and degrades it further to acetate. This striking strategy provides *Shigella* with an abundant supply of a favorable energy source, while preserving host cell viability for prolonged exploitation. The crucial role of acetate metabolism for *Shigella* growth suggests potential new targets for antimicrobial chemotherapy.**

Author contributions: D.K., P.K., J.A.V., S.H., and D.B. designed research; D.K., G.M., M.C., P.C., M.B., O.B., A.W., P.N., N.D., and P.K. performed research; J.L. and R.S. contributed new reagents/analytic tools; D.K., G.M., M.C., P.C., M.B., O.B., A.W., P.N., N.D., J.G., P.K., S.H., and D.B. analyzed data; and D.K., J.A.V., S.H., and D.B. wrote the paper.

The authors declare no conflict of interest.

This article is a PNAS Direct Submission.

Freely available online through the PNAS open access option.

[1]D.K., G.M., and M.C. contributed equally to this work.

[2]To whom correspondence may be addressed. E-mail: david.kentner@gmx.de or dirk.bumann@unibas.ch.

This article contains supporting information online at www.pnas.org/lookup/suppl/doi:10.1073/pnas.1406694111/-/DCSupplemental.

metabolic burden on the infected host cell. Metabolite quantification in infected and uninfected cells identified some metabolites with differential concentrations (Tables S1 and S2), but surprisingly, the energy charge, a measurement of relative ATP, ADP, and AMP levels, did not change significantly on infection (uninfected cells, 0.83 ± 0.03; infected cells, 0.80 ± 0.05). This observation showed that infected cells largely maintain their energy production, despite ongoing exploitation by *Shigella*.

Quantitative metabolite analyses of pathogen-infected host cells encounter the general technical challenge that pathogen and host cell contents are not easily separable within the required time frame. Available separation techniques would inevitably cause a time delay of up to minutes, during which rapid reactions, such as ATP hydrolysis, would substantially alter metabolite concentrations. To avoid such artifacts, we quenched the cell culture immediately and determined combined metabolite concentrations from infected cells and *Shigella*. Because of the much larger volume of human cells compared with *Shigella*, most of these data are probably dominated by host metabolites. As an example, we experimentally determined *Shigella* adenosine phosphate (AXP) contents in various axenic cultures (glucose or pyruvate as sole energy/carbon source provided at 0.1 or 1 g L^{-1}). The results showed that 50 *Shigella* cells contained 0.25–0.69 fmol ATP, 0.19–0.35 fmol ADP, and 0.04–0.05 fmol AMP. Even when subtracting these potential *Shigella* contributions from the combined AXP levels of infected HeLa cells, the HeLa-only AXP values would still yield an energy charge of 0.79 ± 0.02, suggesting a very minor impact of *Shigella* AXP on calculated host cell energy charge values, which was expected based on the different cell volumes of HeLa and *Shigella*.

Various mechanisms could enable infected host cells to maintain their energy charge, despite *Shigella* exploitation. In particular, infected cells might increase nutrient uptake from the extracellular environment (17). However, under the experimental conditions used here, uninfected and infected cells consumed glucose at similar rates (9.0 ± 1.1 vs. 9.3 ± 1.3 fmol/min per cell), whereas uptake of glutamine, another potentially major nutrient for mammalian cells, remained below 0.5 fmol/min per cell.

To determine metabolic fluxes involved in host cell ATP production, we switched unlabeled glucose in the external medium to uniformly labeled (*U*-) ^{13}C glucose and monitored subsequent ^{13}C incorporation in diverse metabolites using mass spectrometry (MS) (Fig. 1*A* and Table S3). Uninfected HeLa cells showed uptake and catabolism of glucose through Embden–Meyerhof and pentose phosphate pathways but very little feeding into tricarboxylic acid (TCA) cycle intermediates, indicating predominant ATP generation through fermentation, which was previously shown for HeLa and other cancer cell lines (18, 19). Interestingly, infected HeLa cells, which contained around 50 rapidly growing *Shigella* at 2.5 h postinfection, had almost

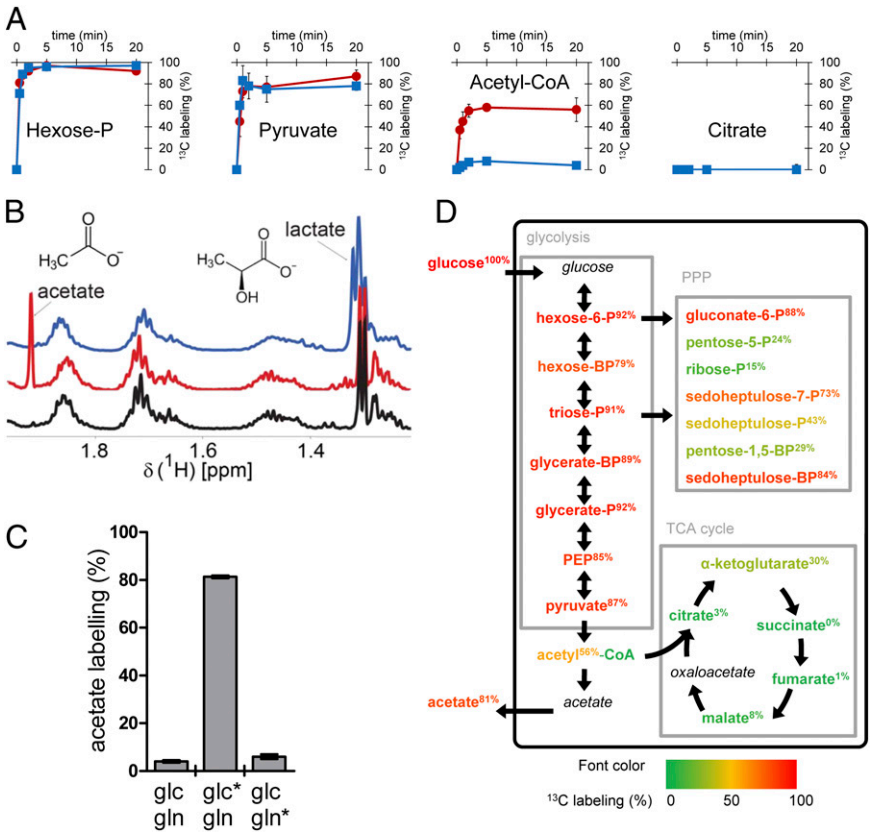

Fig. 1. (*A*) ^{13}C-incorporation kinetics for various metabolites in uninfected (blue) or infected (red) HeLa cells after feeding of *U*-^{13}C glucose. The ^{13}C-labeling percentage is calculated as the fraction of the labeled species (2-^{13}C for acetyl-CoA and *U*-^{13}C for others) relative to the total metabolite pool. Data are represent means and SDs of six independent experiments (Table S3 shows the full dataset). (*B*) Extracellular metabolites before (black) and 3 h after (red) infection as detected by 1D ^{1}H NMR (Fig. S3 shows identification of acetate by 2D [^{13}C,^{1}H] NMR). Uninfected HeLa cells are shown for comparison (blue). The medium contained *U*-^{13}C glucose. (*C*) ^{13}C labeling of extracellular acetate in medium containing *U*-^{13}C–labeled compounds (glc*, glucose; gln*, glutamine) or unlabeled compounds (glc, glucose; gln, glutamine). Data represent means and SDs of three independent experiments. (*D*) Overview of ^{13}C labeling of metabolites from *U*-^{13}C glucose in infected HeLa cells. Font color and superscripts indicate the percentage of the labeled species (2-^{13}C for acetyl-CoA and *U*-^{13}C for others) after 20 min (all intracellular metabolites) or 1 h (acetate) of feeding with ^{13}C glucose. Data represent means from six independent experiments. PPP, pentose phosphate pathway and related metabolites.

identical label incorporation kinetics in Embden–Meyerhof and pentose phosphate pathway intermediates and marginal flux into the TCA cycle. This flux distribution suggested that host cells maintained their energy charge during infection by using the main preexisting energy-producing glycolytic pathways. Proteome comparisons revealed that, in general, host cell enzyme abundance changed little during infection (Fig. S2), arguing against a major reorganization of the host metabolic network during infection. This proteomics result was consistent with previous data on unaltered host cell amino acid biosynthesis during infection with related enteroinvasive *E. coli* (7).

Infection Reroutes Carbon Flux to Acetate Excretion. The apparently minor impact of infection on central host metabolism was surprising, because *Shigella* obviously must redirect major metabolic fluxes and capture abundant metabolites to sustain its rapid proliferation. Indeed, our ^{13}C glucose isotope-tracking experiments showed one remarkable difference between infected and uninfected cells: a substantial fraction (56 ± 11%) of the acetyl moiety in acetyl-CoA was rapidly labeled exclusively in infected cells (Fig. 1*A* and Table S3). Interestingly, this ^{13}C was hardly transferred to TCA cycle intermediates, suggesting metabolization through other pathways. To identify potential end products, we analyzed metabolites in the cell culture medium by NMR spectroscopy. Uninfected cells converted glucose to lactate and pyruvate (Figs. 1*B* and 2*A*), which was expected for this cell line (20). Surprisingly, lactate and pyruvate excretion was completely abolished in *Shigella*-infected cells (Figs. 1*B* and 2*A*). Instead, these cells excreted acetate at a ratio of 2.1 ± 0.3 acetate per consumed glucose (Figs. 1*B* and 2*A* and Fig. S2, identification of acetate by NMR). Experiments using media containing ^{13}C glucose or ^{13}C glutamine showed that most acetate originated from glucose but not glutamine (Fig. 1*C*).

Together, these data showed that, in infected cells, the dominant glycolytic pathways were fully functional but that their entire output was rerouted to acetate (Fig. 1*D*). This finding was in marked contrast to *Shigella*-infected macrophages that become metabolically inactive and rapidly die (21) because of IpaB-mediated pyroptosis (22).

***Shigella* Produces Acetate from Pyruvate.** Acetate is the dominant waste product of rapidly growing *Enterobacteriaceae*, such as *Shigella* and *E. coli* (23). Specifically, *Shigella* uses phosphotransacetylase (PTA) to convert acetyl-CoA to acetyl phosphate and acetate kinase (ACKA) to convert acetyl phosphate and ADP to acetate and ATP. To test the role of this *Shigella* acetate-generating pathway during infection, we constructed *Shigella pta* and *ackA* mutants. Both *Shigella* mutants had substantial intracellular growth defects (40–60% of parental strain) (Fig. 2*B* and Table S4). Complementation of the *pta* mutant with an episomal *pta* allele rescued normal growth, indicating that the *Shigella pta* phenotype was caused by the deletion of *pta*. The reduced mutant growth rates resulted in strongly diminished *Shigella* loads after 3.5 h of infection (13 ± 2 *Shigella pta* and 8 ± 1 *Shigella ackA* per HeLa cell vs. 73 ± 9 parental *Shigella*), consistent with longer generation times. Over an entire day of infection, these longer generation times could lead to some 500,000-fold lower *Shigella* loads for mutants vs. the parental strain (assuming continuous growth). These data show that the acetate pathway is active and essential for normal *Shigella* intracellular growth. Similar data for polarized Caco-2 cells and human umbilical vein endothelial cells (HUVECs) (Table S4) suggested analogous *Shigella* metabolic strategies in a colon epithelial cell line as well as primary human cells.

HeLa cells infected with *Shigella pta* or *ackA* excreted lactate and pyruvate but very little acetate (Fig. 2*A*). These data suggested that most of the acetate excreted from HeLa cells that were infected with the *Shigella* parental strain was a product of

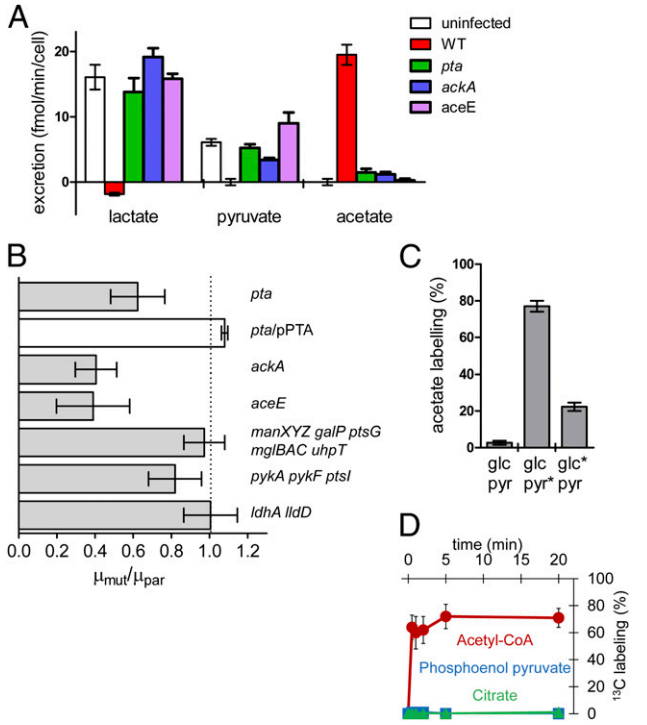

Fig. 2. (*A*) Net metabolite excretion of uninfected HeLa cells and HeLa cells infected with various *Shigella* strains between 2 and 3 h postinfection determined by NMR spectroscopy. Data represent means and SDs of three independent experiments. (*B*) Intracellular generation time of *Shigella* mutant strains (μ_{mut}) relative to the parental strain (μ_{par}; *pta*/pPTA, *Shigella pta* mutant complemented *in trans* with an episomal *pta* allele). A value of 1.0 (dashed line) corresponds to unimpaired growth. Data represent means and SDs of 34–56 replicate wells. Detailed data and statistical analysis are in Table S4. (*C*) ^{13}C labeling of extracellular acetate in medium containing U-^{13}C–labeled compounds (glc*, 25 mM glucose; pyr*, 5 mM pyruvate) or unlabeled compounds (glc, 25 mM glucose; pyr, 5 mM pyruvate). Data represent means and SDs of three independent experiments. (*D*) ^{13}C-incorporation kinetics of acetyl-CoA, phosphoenolpyruvate, and citrate in infected HeLa cells after feeding U-^{13}C pyruvate in the presence of a fivefold excess of unlabeled glucose. Labeling percentage refers to the fraction of 2-^{13}C (acetyl-CoA) or *U*-^{13}C (PEP and citrate) metabolite relative to the total metabolite pool. Data represent means and SDs of three independent experiments (full dataset is in Table S5).

Shigella pyruvate to acetate conversion, which largely depends on a functional PTA–ACKA pathway (23). The low residual acetate production of cells infected with *Shigella pta* or *ackA* mutants could reflect alternative *Shigella* pathways [such as pyruvate oxidation mediated by pyruvate oxidase (POXB)] or host cell activities (23). HeLa cells incubated together with gentamicin-killed *Shigella* excreted no acetate, again consistent with acetate as a product of *Shigella* metabolism.

Together, these data suggest that infected cells switched from lactate excretion to acetate excretion as a result of *Shigella* capturing host metabolites and converting them to acetate primarily through the PTA–ACKA pathway.

Pyruvate Is Taken Up by *Shigella* from the Host Cytosol. To determine potential host metabolites that fuel *Shigella* acetate generation, we mutated additional metabolic genes. *Shigella aceE* deficient for pyruvate dehydrogenase and thus, impaired in conversion of pyruvate to acetyl-CoA showed a strong growth defect and largely abolished acetate production, suggesting that pyruvate was a major source of acetyl-CoA and acetate in *Shigella* (Fig. 2*B* and Table S4).

MICROBIOLOGY

Shigella could obtain this pyruvate directly from the host cell cytoplasm or generate it itself from other host cell metabolites through glycolysis and/or lactate oxidation. A *Shigella manXYZ galP ptsG mglBAC uhpT* mutant unable to use glucose and mannose as well as hexose phosphates exhibited unimpaired growth (Fig. 2*B* and Table S4). A *pykA pykF ptsI* mutant defective for the last step of glycolysis [conversion of phosphoenolpyruvate (PEP) to pyruvate], which cannot grow on any glycolysis intermediate upstream of pyruvate in vitro, had a moderate growth defect (77 ± 10% of the parental strain's intracellular growth rate) (Fig. 2*B* and Table S4). These data indicated the importance of the PEP–pyruvate conversion but also showed substantial growth of *Shigella*, even without the use of any host glycolysis intermediate. This mutant phenotype was consistent with unabated ^{13}C-label incorporation in host cell metabolites from hexose phosphate all of the way down to pyruvate, suggesting at most, minor consumption of host cell intermediates upstream of pyruvate by *Shigella*. These data are in agreement with previous studies showing no growth of closely related *E. coli* on key glycolysis intermediates 3-phosphoglycerate, 2-phosphoglycerate, and phosphoenolpyruvate (24), and toxic effects of excessive uptake of organophosphates (25). Finally, *Shigella ldhA lldD* incapable of lactate utilization also maintained normal growth, arguing against lactate as a critical source of pyruvate (Fig. 2*B* and Table S4). Taken together, these data suggested direct uptake of pyruvate by *Shigella* from the host cell cytoplasm as the main supply route. A major role of pyruvate and its apparently complete conversion into acetate was also consistent with the fact that pyruvate (oxidation state +2) is a highly acetogenic substrate compared with nutrients with a lower oxidation state, such as glucose (23).

Initially, it was surprising that just a few *Shigella* cells could apparently capture the entire glycolysis output of much larger HeLa cells. However, *Shigella* can efficiently use external pyruvate as a sole carbon and energy source. Indeed, NMR spectroscopy revealed that *Shigella* consumed pyruvate in vitro at a rate of 0.35 ± 0.06 fmol min^{-1} per *Shigella* in M9 minimal medium containing 1 mM pyruvate and nicotinic acid and 0.1% tryptic soy broth as supplements. Based on these data, some 50 *Shigella* can indeed consume all pyruvate generated by host metabolism in an infected HeLa cell (around 20 fmol min^{-1}; see above).

Direct validation of *Shigella* pyruvate uptake during intracellular growth would require a mutant with blocked pyruvate uptake. Unfortunately, several yet unidentified high-affinity pyruvate transporters exist in *Shigella*/*E. coli* (26). We deleted multiple tentative candidates [*yhjE* (27); *actP*, a homolog of *mctC* (28); *ycaM* and *ybaT*, putative transporter genes up-regulated in *E. coli* on pyruvate-containing media (29)], but the resulting combination mutant was still able to grow rapidly on pyruvate in vitro, showing the presence of other yet unidentified pyruvate import mechanisms.

As an alternative approach, we added ^{13}C pyruvate to the external medium of infected HeLa cells and tracked the labeled carbon. NMR analysis of the extracellular medium revealed efficient conversion of ^{13}C pyruvate to ^{13}C acetate, even in the presence of an excess of unlabeled glucose (Fig. 2*C*), consistent with preferred use of pyruvate over glucose and glycolysis pathway intermediates. Indeed, the only detectable intracellular metabolite that rapidly acquired substantial amounts of ^{13}C in infected cells was acetyl-CoA, whereas directly adjacent metabolites PEP and citrate were not labeled or labeled at much lower rate (Fig. 2*D* and Table S5). Their poor labeling rules out Embden–Meyerhof and pentose phosphate pathways or TCA cycle intermediates as relevant sources of the strongly labeled excreted acetate and supports a direct conversion of host-derived pyruvate to acetyl-CoA and acetate by *Shigella*.

Together, these data suggest major *Shigella* nutrient use through a short pathway: pyruvate (host cytoplasm) → pyruvate (*Shigella*) → acetyl-CoA (*Shigella*) → acetyl-phosphate (*Shigella*) → acetate (*Shigella*) → acetate (host cytoplasm) → acetate (medium) (Fig. 3). For each pyruvate molecule, this pathway yields one ATP in the conversion of acetyl-phosphate to acetate. Because one molecule of glucose is essentially fully converted into two excreted acetate molecules, this pathway predominantly provides energy, but not carbon, for *Shigella* growth. The limited role of pyruvate as a carbon source might explain why this major pathway escaped detection in previous metabolic studies of related pathogens using methods focusing on pathogen biomass incorporation (10).

Intracellular *Shigella* Consume Oxygen by Respiration. Oxidation of glucose to pyruvate and pyruvate to acetate yields reducing equivalents that might, in part, be used for *Shigella* biosynthetic pathways, such as lipogenesis. In addition, infected cells consumed oxygen at a rate of 0.07 ± 0.02 fmol/min per *Shigella*, whereas uninfected cells had undetectable oxygen consumption in our assay. This oxygen consumption was mostly caused by *Shigella* respiration, because cells infected with *Shigella ubiC menA* (lacking ubiquinone and menaquinone required for aerobic respiration) consumed much less oxygen (0.003 ± 0.001 fmol/min per *Shigella*). This observation is consistent with commonly observed active respiration during acetate production in *Enterobacteriaceae* (23). Additional work is required to identify which of the many potential intermediate electron donors/acceptors are involved in the various host and *Shigella* redox reactions.

Additional Nutrients Support *Shigella* Growth. In addition to the major energy source pyruvate, *Shigella* might obtain other nutrients from the host cell cytoplasm to meet its biomass demands. We analyzed *Shigella* mutants with utilization defects for 18 diverse metabolites that are known to be available in human cell cytoplasm (30). However, all mutants except one had growth rates indistinguishable from the parental strain (Tables S6 and S7). The weak but significant growth defect of *fadD fadK* suggests a potential small contribution of host fatty acids to *Shigella* growth. We also analyzed growth phenotypes of 11 auxotrophic *Shigella* mutants that depend on external supplementation of specific nutrients for growth (Tables S6 and S7). High intracellular growth rates of these auxotrophs showed *Shigella* access to diverse amino acids in sufficient amounts to fully meet their respective *Shigella* biomass needs, which was previously observed for closely related pathogens (10). Asparagine, proline, and purine nucleosides were also available but only in limiting amounts, requiring additional *Shigella* biosynthesis for full

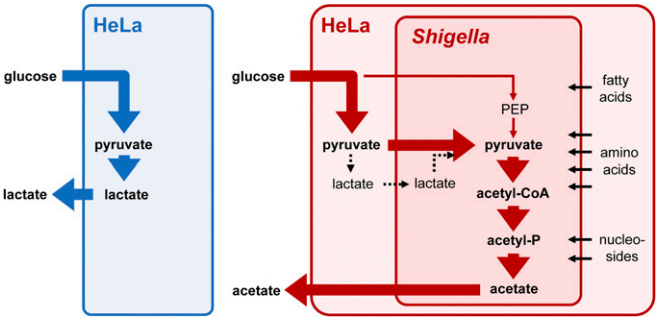

Fig. 3. Metabolic overview of *Shigella*-infected HeLa cells. Uninfected cells (blue) convert glucose to lactate. In infected cells (red), *Shigella* takes up glucose-derived pyruvate from the host cytoplasm and converts it to acetate, which is excreted into the environment. In addition, *Shigella* uses host fatty acids, amino acids, and purine nucleosides. Thick and thin arrows indicate major and minor carbon flux routes, respectively. The dashed arrows represent reactions not supported by available evidence.

growth. Availability of these (and possibly, additional) diverse nutrients represented another important contribution to support vigorous intracellular *Shigella* growth. However, compared with the massive throughput of pyruvate use, uptake of additional nutrients for *Shigella* biomass production must be rather low: based on acetate excretion, each *Shigella* consumed, on average, 1.2 pg pyruvate but generated total new biomass of only 0.4 pg (31) within one generation time (37 min).

We incorporated our data for *Shigella* pyruvate consumption, respiration, and additional biomass supplementation in an in silico genome-scale metabolic model of closely related *E. coli* (32). According to this model, the measured fluxes would enable *Shigella* growth with generation times in the range of 33–54 min (based on error margins of the underlying experimental data), which is in good agreement with our experimentally determined generation time of 37 ± 4 min, showing that nutrients identified in this study can largely explain the outstandingly rapid intracellular *Shigella* growth as one precondition for the rapid and dramatic disease progression in dysentery.

Discussion

Rapid disease progression in bacillary dysentery is the result of vigorous *Shigella* growth in gut epithelial cells. In addition to a large number of virulence factors that interfere with host signaling networks, this fast growth requires massive *Shigella* exploitation of host metabolism for high-flux nutrient supply. However, infected cells remain viable for several hours until they contain more than 100 bacteria. In this study, we show that *Shigella* does not affect the main host cell energy production pathways—Embden–Meyerhof and pentose phosphate pathways—but instead, consumes their entire output at the level of pyruvate. For this purpose, *Shigella* uses a short pyruvate-to-acetate pathway that *Enterobacteriaceae* typically use during rapid growth under nutrient-rich conditions (23). *S. flexneri* cannot reuse acetate later, because it lacks acetyl-CoA synthetase that is present in closely related *E. coli* (33).

This pathway generates only a single ATP for each pyruvate molecule (and some additional ATP through oxidation of NADH), and it is far less efficient in terms of ATP generation compared with the TCA cycle (up to 14 ATP per pyruvate) that predominates under nutrient-poor conditions. However, the low-yield acetate pathway has lower enzyme costs and membrane space requirements and can operate at much faster rates compared with low-throughput, high-yield TCA cycle/oxidative phosphorylation, which requires bulky enzymatic machinery in the bacterial inner membrane. The acetate pathway can, thus, cope with high nutrient supply rates that would saturate the respiratory chain (overflow metabolism) (34). Similar switches to low-yield/high-rate pathways are observed for many microbial cells (Crabtree effect) (23) as well as cancer cells (Warburg effect) (20) during rapid growth.

The use of abundant pyruvate predominantly through this low-yield, high-speed acetate pathway represents a typical metabolic pattern of *Enterobacteriaceae* in general (23). Interestingly, this default pathway could offer several additional important benefits to *Shigella* during intracellular growth in infected human cells: (*i*) use of a favorable abundant energy source, pyruvate, at high rates; (*ii*) exploitation of the dominant preexisting host metabolic pathways as high-flux supply lines without requiring major host cell metabolism alterations that could cause delays and limit supply; and (*iii*) preservation of host cell energy charge by glycolytic ATP generation, allowing extended host cell survival, despite vigorous exploitation. Taken together, a short metabolic pathway that is commonly present in many bacteria enables *Shigella* to efficiently exploit major nutrient supply routes in infected host cells. This preadaptation might explain why *Shigella* can thrive as a voracious pathogen with only minor metabolic adaptations to the host cell intracellular environment compared with closely related extracellular commensals (33, 35). In addition to the major energy source pyruvate, *Shigella* accessed diverse host metabolites for direct biomass incorporation. Computational modeling revealed that all these nutrients together were sufficient to support the experimentally observed rapid *Shigella* intracellular growth.

An important caveat of our study was the use of cancer cell lines as host cells that ferment glucose to lactate to satisfy their energy needs (the Warburg effect). Dysentery is a disease of the colon, and the epithelial cells in this location, the colonocytes, have a different metabolism. Some 80% of ATP produced in colonocytes comes from mitochondrial oxidation of butyrate, which is derived from gut microbiota. However, experiments with germ-free mice have shown that, in the absence of microbiota-derived butyrate, colonocytes switch from burning butyrate to fermenting glucose to lactate (36). It is possible that the flushing action of diarrhea during dysentery removes much of the microbiota, thereby lowering butyrate levels in the colon and triggering colonocyte metabolism similar to HeLa cell metabolism in our in vitro model. Additional studies are required to clarify this issue.

Comprehensive quantitative data on pathogen nutrition, metabolism, and growth in host environments are largely lacking. However, comparison of the *Shigella* data with our recent study on *Salmonella enterica* metabolism in a mouse typhoid fever model (37) reveals commonalities and striking differences. *Shigella*, like *Salmonella* and many other pathogens (37), exploits the fact that most biomass components are readily available in infected host environments. Uptake of these biomass components can save substantial biosynthesis costs. However, *Shigella* has access to a high-flux supply for pyruvate that provides sufficient energy to drive fast growth, whereas intracellular *Salmonella* has access to many diverse but only scarce energy sources that together just support slow nutrient-limited growth (37). This striking difference may reflect the fact that *Shigella* reside directly in the host cytoplasm, whereas intracellular *Salmonella* are surrounded by a phagosomal membrane with apparently poor permeability in macrophages (their main target cell type during systemic infections). Additional studies with other pathogens might clarify the general relevance of these distinct metabolic patterns.

Although host pyruvate supply enables vigorous *Shigella* proliferation, the heavy dependence on pyruvate metabolism makes *Shigella* also vulnerable to metabolic perturbation. Indeed, our mutant data for the corresponding enzymes show dramatically reduced *Shigella* loads compared with the parental strain, even within short infection times. The residual slow growth of these mutants and their altered waste product spectrum show that *Shigella* can use alternative pathways, such as pyruvate oxidase, but these pathways are far less efficient for supporting growth as expected (23). Importantly, the key enzymes phosphotransacetylase (PTA) and acetate kinase (ACKA) have no human homologs, suggesting that specific inhibition of *Shigella* enzymes without adverse effects on human metabolism might be possible. *Shigella* acetate metabolism enzymes could, thus, represent promising targets to control bacillary dysentery.

Materials and Methods

Strains and Plasmids. HeLa Kyoto cells (38) and HUVECs were provided by Cécile Arrieumerlou and Claudia Mistl (Biozentrum, University of Basel). Caco-2 cells (ATCC-HTB-37) were obtained from the American Type Culture Collection. *S. flexneri* 2a 2457T *icsA* was provided by M. B. Goldberg (Massachusetts General Hospital, Boston). All mutants in this work were derived from this *icsA* strain (referred to as the parental strain). Mutants were constructed as described (39) using a λ-red recombinase-mediated allelic replacement system introducing a flippase recognition target sites-flanked chloramphenicol resistance marker (40) followed by purification using phage P1 transduction. Combinations of multiple deletions were made by P1 transduction into mutants, in which the chloramphenicol resistance was removed using flippase. For complementation of the *pta* mutant, we cloned *pta* together with its native promoter (intergenic region upstream of the *ackA-pta* operon) on a medium copy number plasmid (pA15 ori). All strains

carried plasmid pNF106 (SC101 ori) for doxycycline/anhydrotetracycline-inducible expression of *gfp* (39).

Labeled Nutrients. [*U*-99% ^{13}C]-labeled glucose, [*U*-99% ^{13}C; *U*-99% ^{15}N]-labeled glutamine, and [*U*-99% ^{13}C]-labeled pyruvate were purchased from Cambridge Isotopes Laboratories.

***Shigella* Infections.** HeLa cells, CaCo-2 cells, and HUVECs were infected with polylysine-treated *Shigella*. After 30 min, cells were washed and treated with gentamicin. Intracellular growth of GFP-expressing *Shigella* was determined using flow cytometry and plating. Protocols for infections and growth determination are described in detail in *SI Materials and Methods*.

Proteomics of Infected Cells. Cells were harvested, digested with trypsin/chymotrypsin, and analyzed by MS as described in *SI Materials and Methods*.

Measurement of Intracellular Metabolites by MS. Uninfected and infected cells were quenched with acetonitrile/methanol/formic acid. Samples were analyzed by MS. Detailed protocols are described in *SI Materials and Methods*.

Measurement of Glucose Uptake Rates. Glucose consumption was determined using the EnzyChrom Glucose Assay Kit (Bioassay Systems) as described in *SI Materials and Methods*.

Measurement of Excreted Extracellular Metabolites. Supernatants of uninfected and infected cells were analyzed by 1D ^{1}H NMR spectroscopy as described in *SI Materials and Methods*.

Oxygen Consumption Measurements. Oxygen consumption of infected and uninfected cells was determined using Oxoplates (OP96C; PreSens) and a fluorescent plate reader as described in *SI Materials and Methods*.

Modeling of Intracellular *Shigella* Metabolism. Experimental metabolite uptake rates and mutant phenotypes were combined with a modified *E. coli* metabolism reconstruction (32) to model intracellular *Shigella* metabolism using Flux-Balance Analysis as described in *SI Materials and Methods*.

ACKNOWLEDGMENTS. We thank M. B. Goldberg (Massachusetts General Hospital) as well as Cécile Arrieumerlou and Claudia Mistl (Biozentrum, University of Basel) for providing materials, Nicole Freed (Biozentrum, University of Basel) for help with live cell imaging, Philipp Christen (Eidgenössiche Technische Hochschule Zürich) for support with sampling and HPLC-MS, Claudia Fortes and Philipp Schläfli (Functional Genomics Center Zurich) for assistance in proteomic analysis, and Endre Laczko and Tshering Altherr (Functional Genomic Center Zurich) for support in GC-MS. Funding was provided by SystemsX, The Swiss Initiative in Systems Biology (Project "BattleX").

1. DuPont HL, Levine MM, Hornick RB, Formal SB (1989) Inoculum size in shigellosis and implications for expected mode of transmission. *J Infect Dis* 159(6):1126–1128.
2. Schroeder GN, Hilbi H (2008) Molecular pathogenesis of *Shigella* spp.: Controlling host cell signaling, invasion, and death by type III secretion. *Clin Microbiol Rev* 21(1):134–156.
3. Perdomo OJ, et al. (1994) Acute inflammation causes epithelial invasion and mucosal destruction in experimental shigellosis. *J Exp Med* 180(4):1307–1319.
4. Phalipon A, Sansonetti PJ (2007) *Shigella*'s ways of manipulating the host intestinal innate and adaptive immune system: A tool box for survival? *Immunol Cell Biol* 85(2):119–129.
5. Campbell-Valois FX, et al. (2014) A fluorescent reporter reveals on/off regulation of the *Shigella* type III secretion apparatus during entry and cell-to-cell spread. *Cell Host Microbe* 15(2):177–189.
6. Ray K, Marteyn B, Sansonetti PJ, Tang CM (2009) Life on the inside: The intracellular lifestyle of cytosolic bacteria. *Nat Rev Microbiol* 7(5):333–340.
7. Götz A, Eylert E, Eisenreich W, Goebel W (2010) Carbon metabolism of enterobacterial human pathogens growing in epithelial colorectal adenocarcinoma (Caco-2) cells. *PLoS ONE* 5(5):e10586.
8. Andersen KB, von Meyenburg K (1980) Are growth rates of *Escherichia coli* in batch cultures limited by respiration? *J Bacteriol* 144(1):114–123.
9. Fuchs TM, Eisenreich W, Heesemann J, Goebel W (2012) Metabolic adaptation of human pathogenic and related nonpathogenic bacteria to extra- and intracellular habitats. *FEMS Microbiol Rev* 36(2):435–462.
10. Eisenreich W, Dandekar T, Heesemann J, Goebel W (2010) Carbon metabolism of intracellular bacterial pathogens and possible links to virulence. *Nat Rev Microbiol* 8(6):401–412.
11. Rohmer L, Hocquet D, Miller SI (2011) Are pathogenic bacteria just looking for food? Metabolism and microbial pathogenesis. *Trends Microbiol* 19(7):341–348.
12. Abu Kwaik Y, Bumann D (2013) Microbial quest for food in vivo: 'Nutritional virulence' as an emerging paradigm. *Cell Microbiol* 15(6):882–890.
13. Kafsack BF, Llinás M (2010) Eating at the table of another: Metabolomics of host-parasite interactions. *Cell Host Microbe* 7(2):90–99.
14. Bernardini ML, Mounier J, d'Hauteville H, Coquis-Rondon M, Sansonetti PJ (1989) Identification of icsA, a plasmid locus of *Shigella flexneri* that governs bacterial intra- and intercellular spread through interaction with F-actin. *Proc Natl Acad Sci USA* 86(10):3867–3871.
15. Goldberg MB, Theriot JA (1995) *Shigella flexneri* surface protein IcsA is sufficient to direct actin-based motility. *Proc Natl Acad Sci USA* 92(14):6572–6576.
16. Sansonetti PJ, Ryter A, Clerc P, Maurelli AT, Mounier J (1986) Multiplication of *Shigella flexneri* within HeLa cells: Lysis of the phagocytic vacuole and plasmid-mediated contact hemolysis. *Infect Immun* 51(2):461–469.
17. Mantis N, Prévost MC, Sansonetti P (1996) Analysis of epithelial cell stress response during infection by *Shigella flexneri*. *Infect Immun* 64(7):2474–2482.
18. Munger J, et al. (2008) Systems-level metabolic flux profiling identifies fatty acid synthesis as a target for antiviral therapy. *Nat Biotechnol* 26(10):1179–1186.
19. Goldberg EB, Colowick SP (1965) The role of glycolysis in the growth of tumor vells. 3. Lactic dehydrogenase as the site of action of oxamate on the growth of cultured cells. *J Biol Chem* 240:2786–2790.
20. Vander Heiden MG, Cantley LC, Thompson CB (2009) Understanding the Warburg effect: The metabolic requirements of cell proliferation. *Science* 324(5930):1029–1033.
21. Sansonetti PJ, Mounier J (1987) Metabolic events mediating early killing of host cells infected by *Shigella flexneri*. *Microb Pathog* 3(1):53–61.
22. Senerovic L, et al. (2012) Spontaneous formation of IpaB ion channels in host cell membranes reveals how *Shigella* induces pyroptosis in macrophages. *Cell Death Dis* 3:e384.
23. Wolfe AJ (2005) The acetate switch. *Microbiol Mol Biol Rev* 69(1):12–50.
24. Saier MH, Jr., Wentzel DL, Feucht BU, Judice JJ (1975) A transport system for phosphoenolpyruvate, 2-phosphoglycerate, and 3-phosphoglycerate in *Salmonella typhimurium*. *J Biol Chem* 250(13):5089–5096.
25. Kadner RJ, Murphy GP, Stephens CM (1992) Two mechanisms for growth inhibition by elevated transport of sugar phosphates in *Escherichia coli*. *J Gen Microbiol* 138(10):2007–2014.
26. Kreth J, Lengeler JW, Jahreis K (2013) Characterization of pyruvate uptake in *Escherichia coli* K-12. *PLoS ONE* 8(6):e67125.
27. Huhn S (2011) Identifikation und Charakterisierung von bakteriellen Carbonsäure-Transportern. PhD thesis (Cologne Univ, Cologne, Germany).
28. Jolkver E, et al. (2009) Identification and characterization of a bacterial transport system for the uptake of pyruvate, propionate, and acetate in *Corynebacterium glutamicum*. *J Bacteriol* 191(3):940–948.
29. Göhler AK, et al. (2011) More than just a metabolic regulator—elucidation and validation of new targets of PdhR in *Escherichia coli*. *BMC Syst Biol* 5:197.
30. Wishart DS, et al. (2013) HMDB 3.0—The Human Metabolome Database in 2013. *Nucleic Acids Res* 41(Database issue):D801–D807.
31. Neidhardt FC (1996) *Escherichia coli and Salmonella: Cellular and Molecular Biology* (ASM Press, Washington, DC), 2nd Ed.
32. Feist AM, et al. (2007) A genome-scale metabolic reconstruction for *Escherichia coli* K-12 MG1655 that accounts for 1260 ORFs and thermodynamic information. *Mol Syst Biol* 3:121.
33. Monk JM, et al. (2013) Genome-scale metabolic reconstructions of multiple *Escherichia coli* strains highlight strain-specific adaptations to nutritional environments. *Proc Natl Acad Sci USA* 110(50):20338–20343.
34. van Hoek MJ, Merks RM (2012) Redox balance is key to explaining full vs. partial switching to low-yield metabolism. *BMC Syst Biol* 6:22.
35. Bliven KA, Maurelli AT (2012) Antivirulence genes: Insights into pathogen evolution through gene loss. *Infect Immun* 80(12):4061–4070.
36. Donohoe DR, Wali A, Brylawski BP, Bultman SJ (2012) Microbial regulation of glucose metabolism and cell-cycle progression in mammalian colonocytes. *PLoS ONE* 7(9):e46589.
37. Steeb B, et al. (2013) Parallel exploitation of diverse host nutrients enhances *Salmonella* virulence. *PLoS Pathog* 9(4):e1003301.
38. Neumann B, et al. (2006) High-throughput RNAi screening by time-lapse imaging of live human cells. *Nat Methods* 3(5):385–390.
39. Mary C, et al. (2012) Functional identification of APIP as human *mtnB*, a key enzyme in the methionine salvage pathway. *PLoS ONE* 7(12):e52877.
40. Datsenko KA, Wanner BL (2000) One-step inactivation of chromosomal genes in *Escherichia coli* K-12 using PCR products. *Proc Natl Acad Sci USA* 97(12):6640–6645.